Insights into a tectonic swarm-like seismic Sequence related to a Low Angle Normal Fault system from a Seismic Catalog enhanced by Template Matching

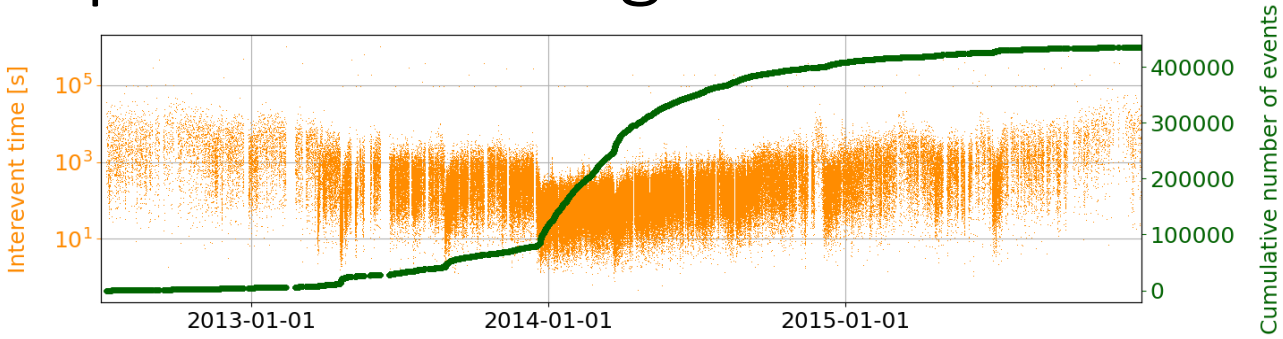

David Essing & Piero Poli

EGU 2021

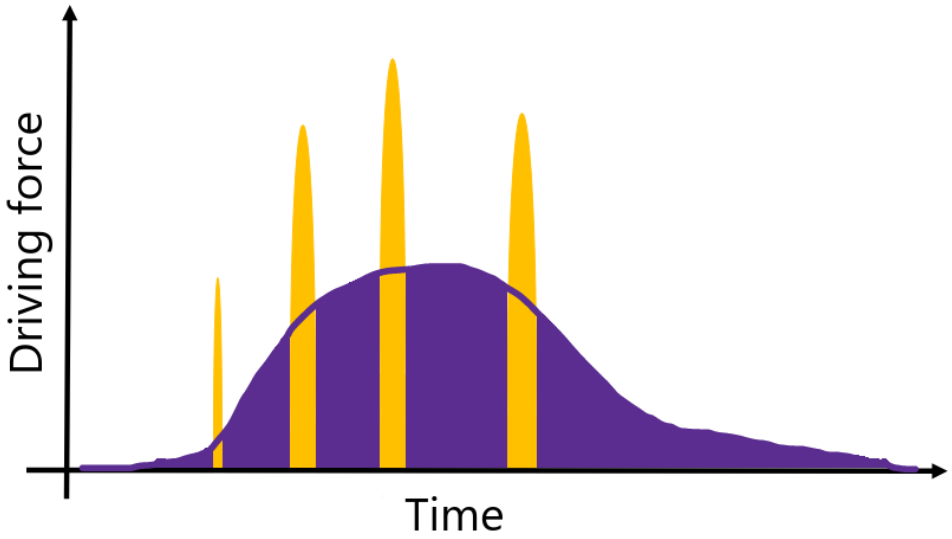

The Alto-Tiberina Fault System

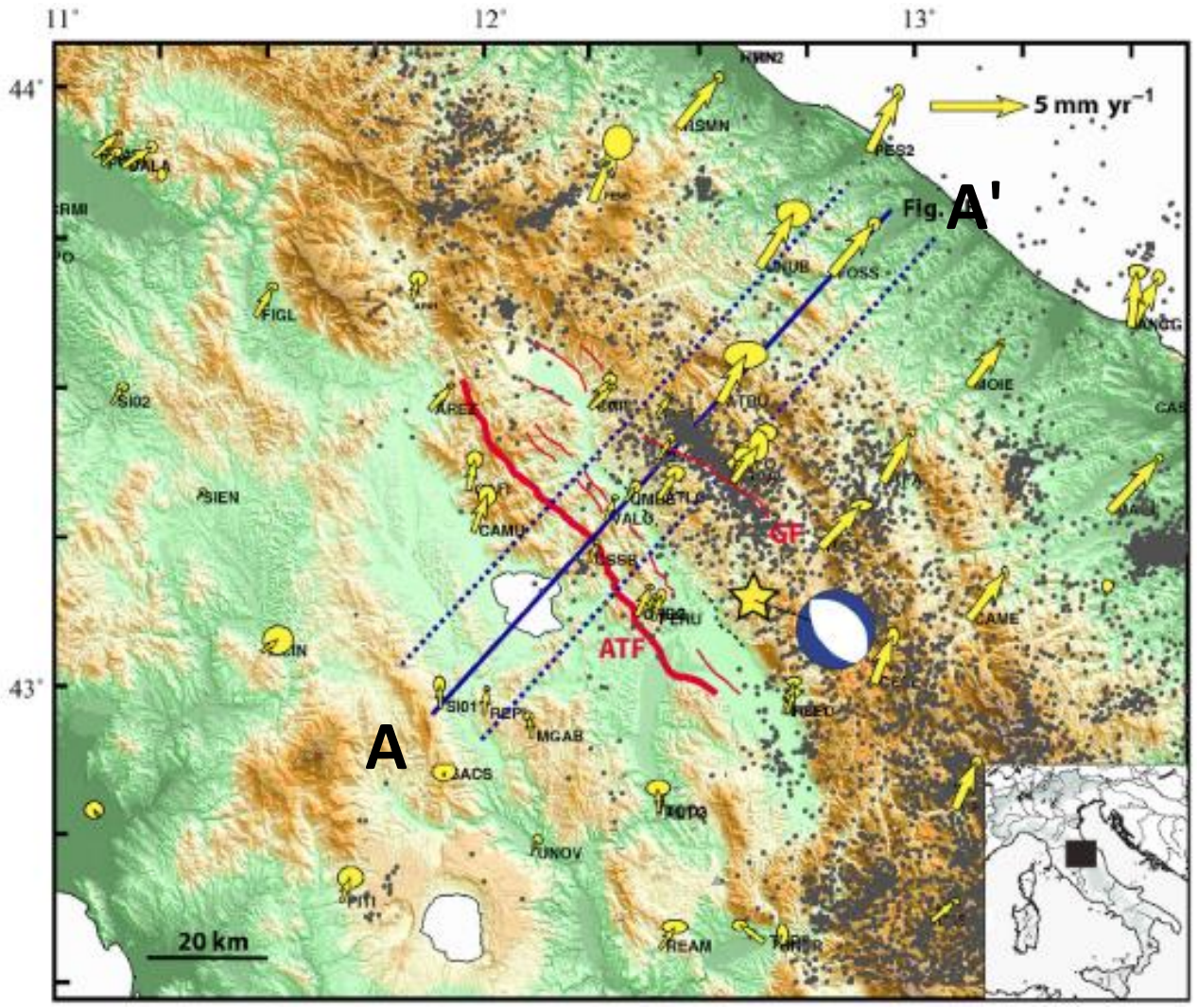

Vadacca et al. (2016)

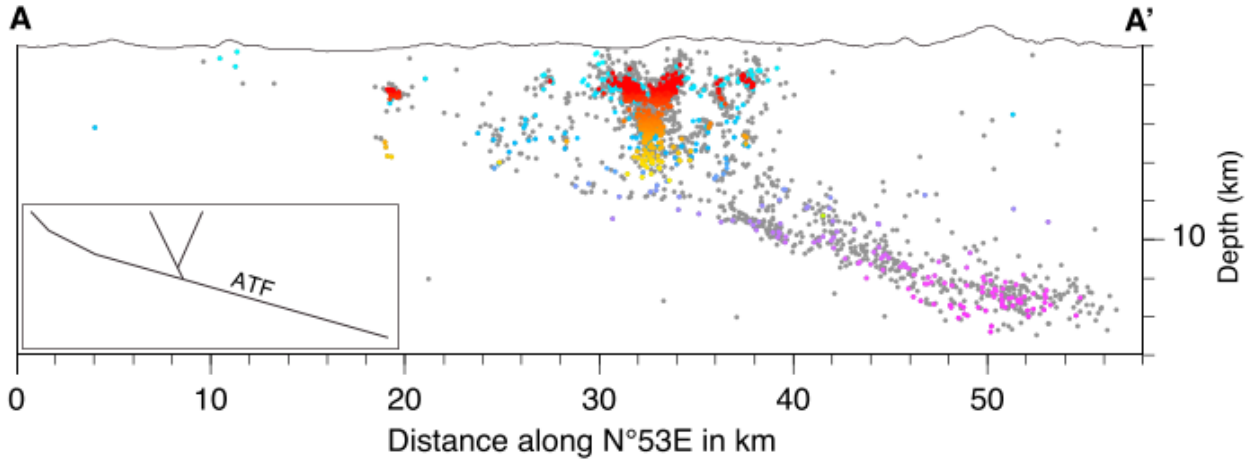

Gualandi et al. (2017)

- **Low Angle Normal Fault** (LANF) at depths **below 3-5 km**
  - **Micro-seismicity** (ML< 2.4), 2.2 events/day
  - within ≈ 1 km thick dipping fault
  - indicates **creep** (Anderlini et al., 2016)
- **Shallow** portion of the **LANF**
  - no seismicity detected (indicating **locked** part)
  - capable of generating M6.5+ (Anderlini et al., 2016)
- Faults in the **hanging wall**
  - **Normal faults** (more favorably oriented to frictional slip)
  - **MS < 5.2 in 1984** (yellow star, Haessler et al. 1988)

Alto Tiberina Near Fault Observatory (TABOO) & Initial catalog

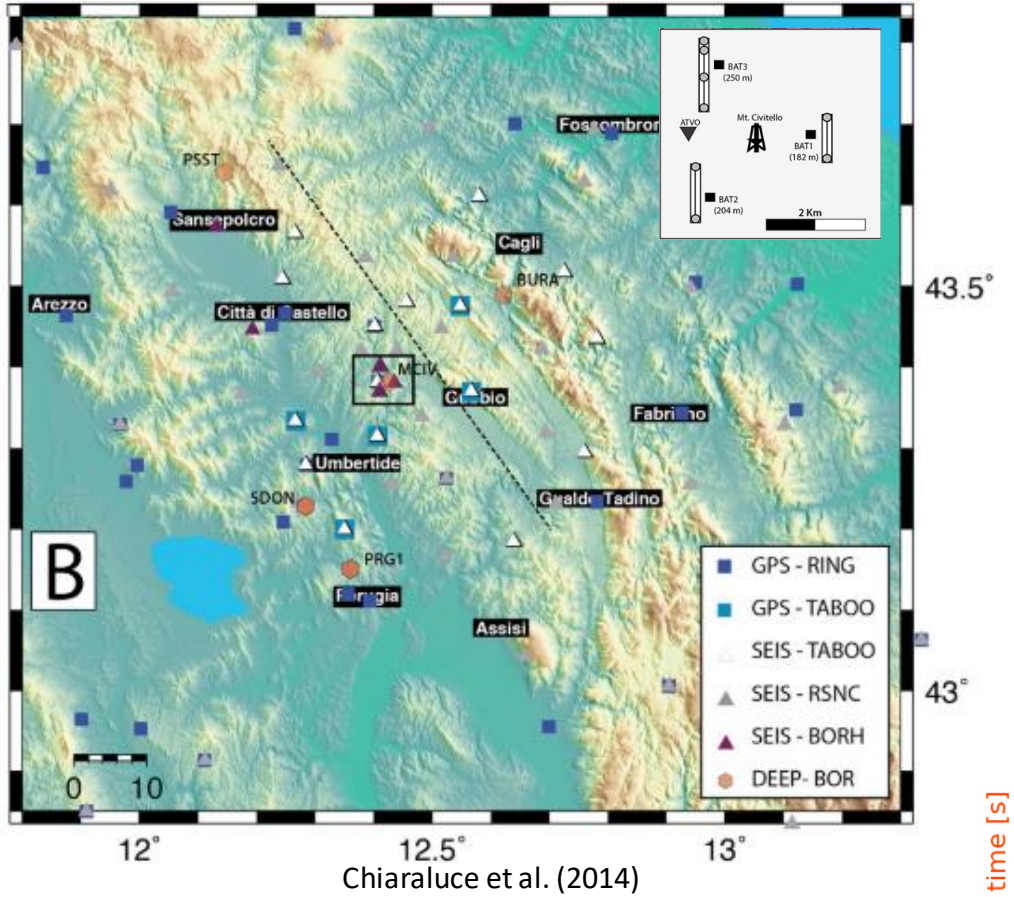

Chiaraluce et al. (2014)

The TABOO infrastructure consists of **multi-sensor stations** (surface-, **borehole-seismometers** and **GPS sensors**), to monitor the seismicity and the deformation of the Alto Tiberina fault (ATF) system.

In late 2013, a **swarm-like seismic sequence** started with an increased rate of seismicity. Within this period several **events with M > 3** occurred in the hanging wall of the ATF. As their related **aftershocks** can **only account for a small portion** of the seismicity, the driving mechanism of the swarm-like sequence is still under debate**.** In GPS data **Gualandi et al. (2017)** extract a signal indicating **aseismic deformation** related to the swarm-like sequence.

In order to characterize the seismicity and the related aseismic deformation in terms of small scale dynamics we extend an existing earthquake catalog consisting of **34,923 events** (Chiaraluce et al.,2019) by combining high quality seismic data from **borehole seismometers** with **template matching**.

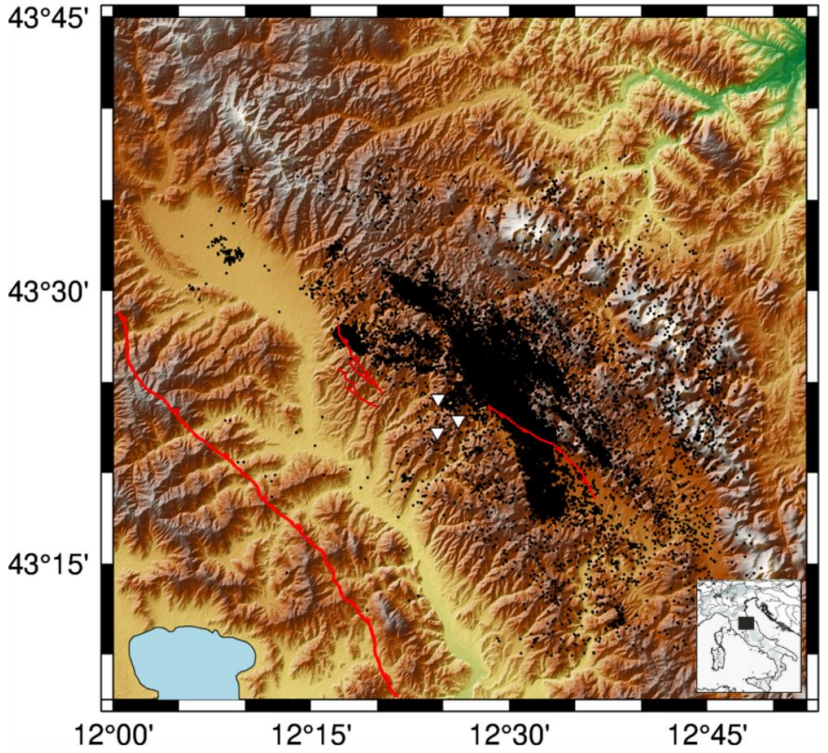

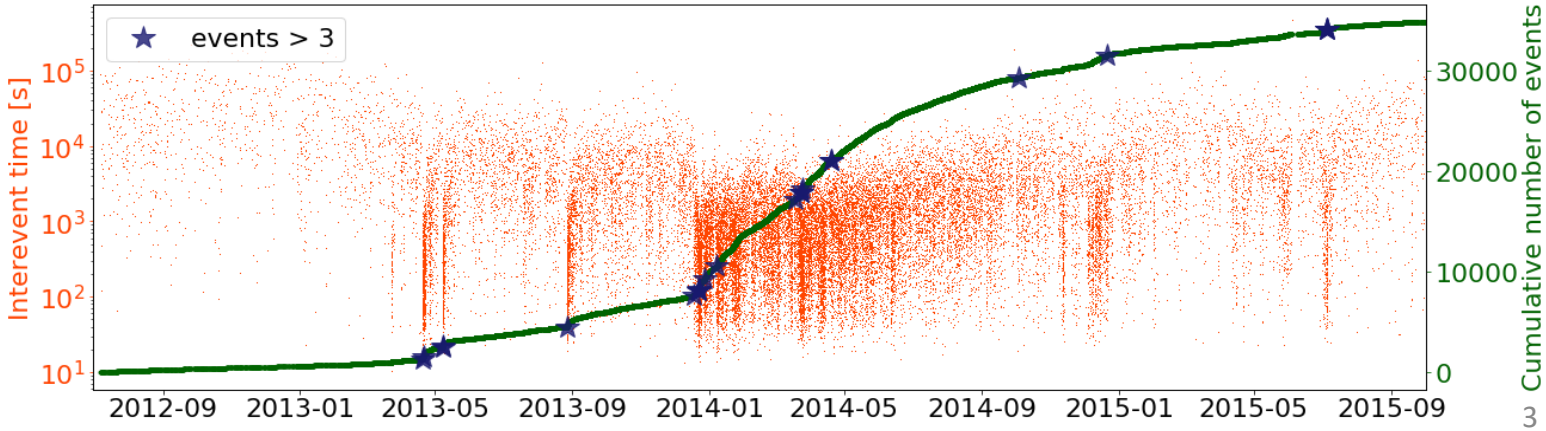

Template matching on seismic data from boreholes

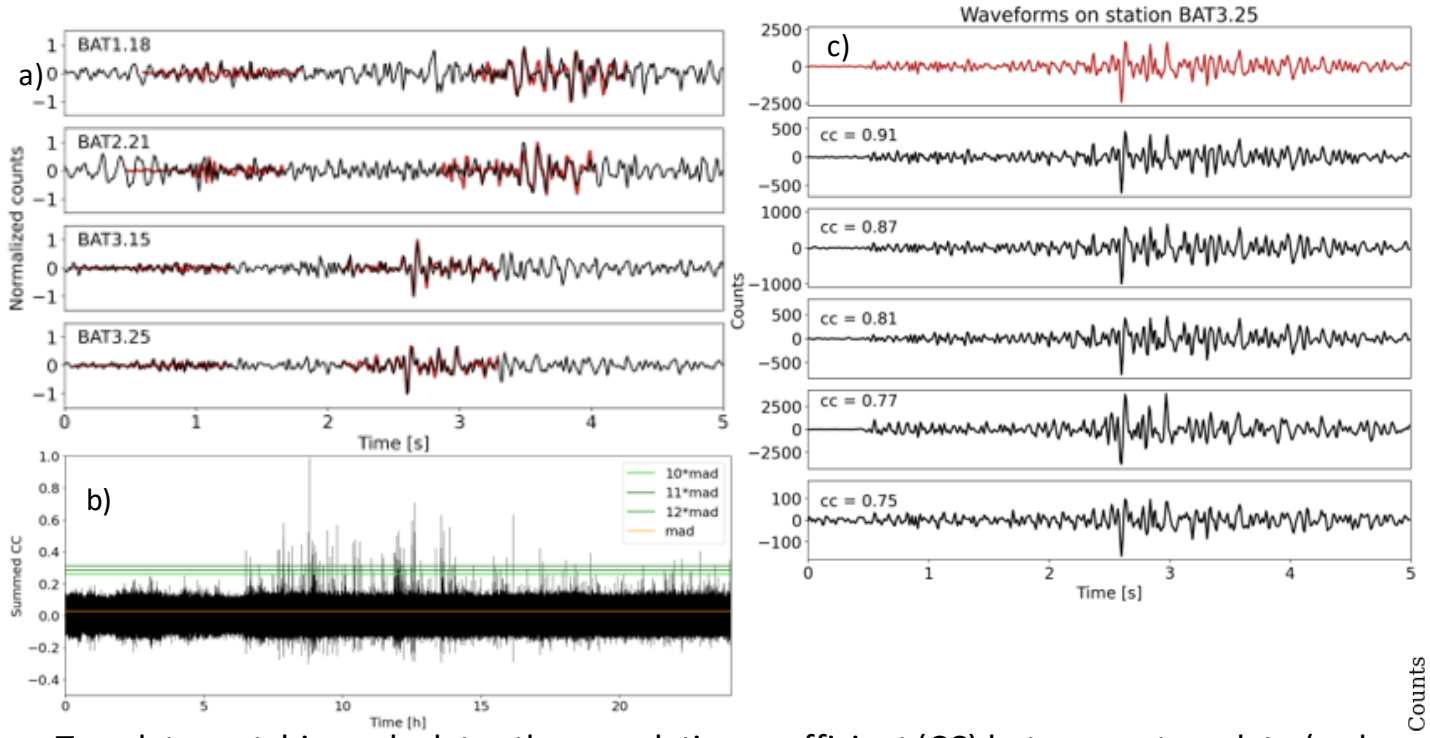

In this study, we make use of continuous **seismic data** from **borehole seismometers** (black waveforms, white triangles (map)) (filtered between **5-49 Hz)** as they are sensitive to small events. The waveforms plotted origin from an event (black dot in map) near the borehole station array.

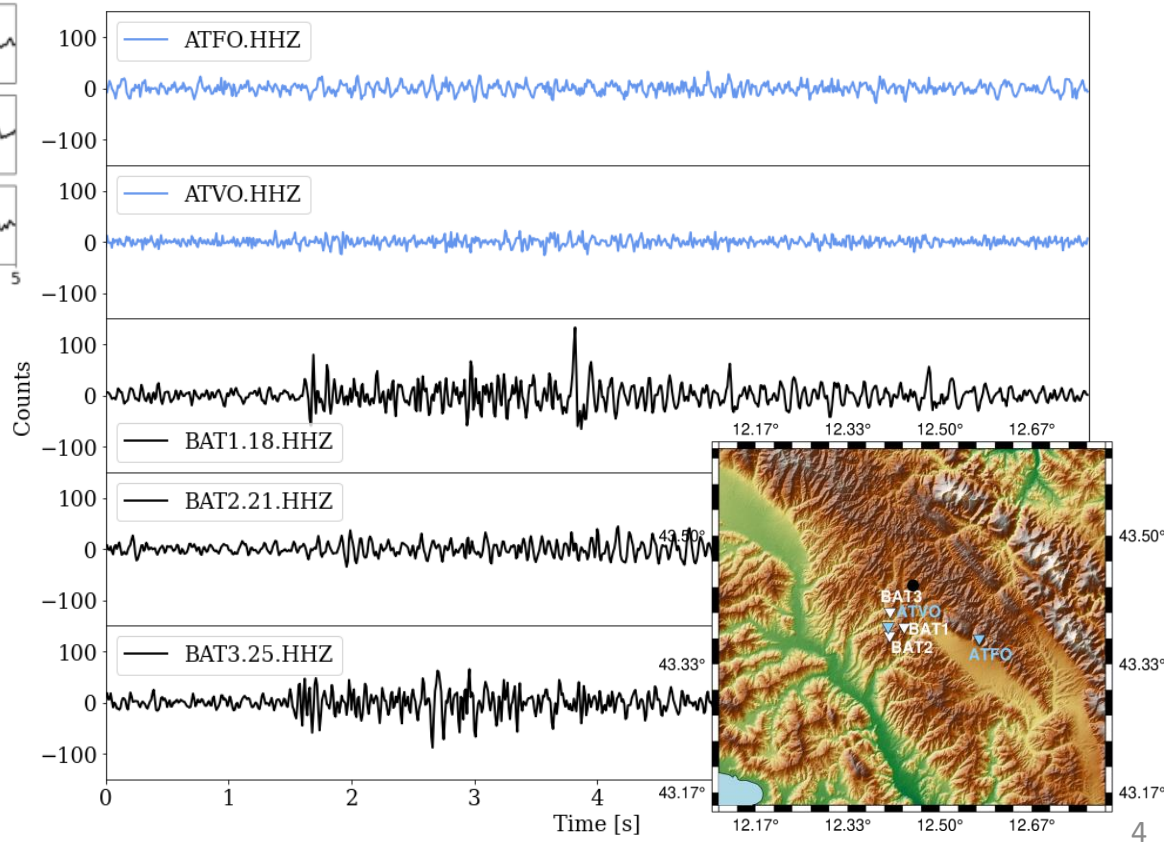

Template matching calculates the correlation coefficient (CC) between a template (red waveform a), **1.2 s window length**) and continuous seismic data (black waveform a)) and eventually sums it over the number of stations used (b)). To turn that approach into an **earthquake detector**, we establish a detection threshold of 10 times the median absolute deviation (MAD) of the summed CCs of one day. We declare every time-window that exceeds this threshold as a new detection.

Using this approach we detect waveforms with a high similarity between them and their detecting template (c)), which implies a **similar mechanism** responsible for the wave radiation. As we take the move-out of every template into account we only detect events close to the templates location.

Declustering of new detected events and quality threshold

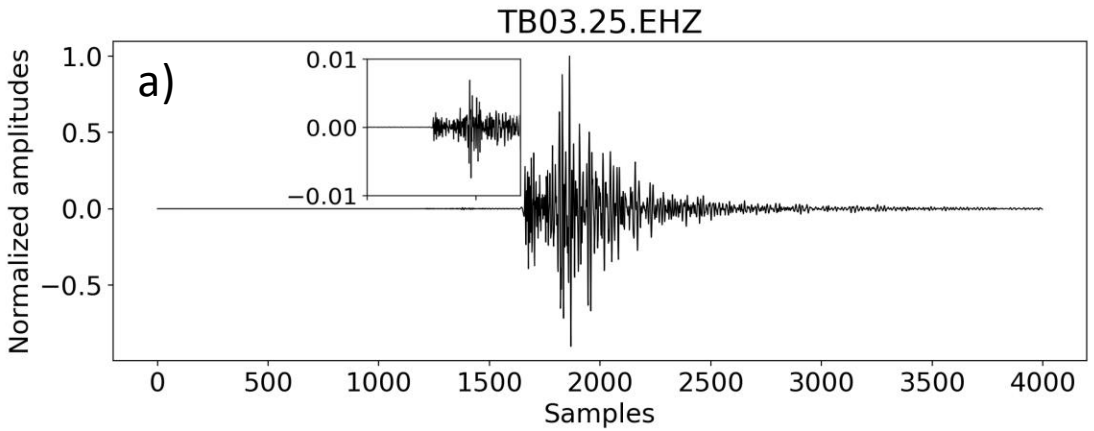

The resulting catalog is **declustered** in time to exclude double detections (same new event detected by several templates) which usually have inter-event times < 1s. At the same time we want to include events with small inter-event times (like shown in a)) where a small event is preceding a larger event by around 3s.

Eventually we keep events that have a **mean inter-event arrival time** at the station array **larger than 1.2s** (this is the window length of a template).

In this study we include detections into our new catalog if their CC exceeds 10 times the MAD on the day of detection. In the Figure below all detections made by a certain template (upper waveform) are shown, sorted by a decreasing CC. Events above the **upper green horizontal line have values > 12*MAD**. Here the peak of the s-phase is clearly visible. Below the **l**ower green vertical line (11*MAD) the s-phase fades out. The waveform in the lower panel indicates the last event detected, having a CC of around 10*MAD. In the following results we will consider only events which have a **CC > 12*MAD**.

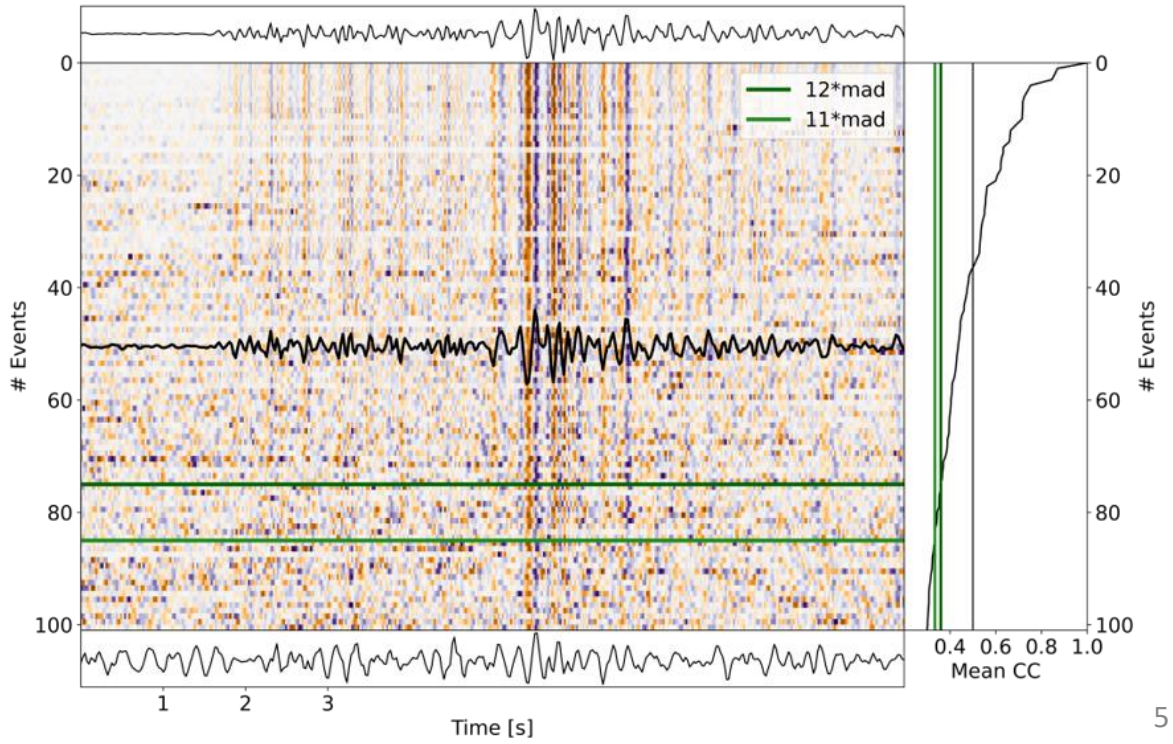

Results – Enhanced catalog

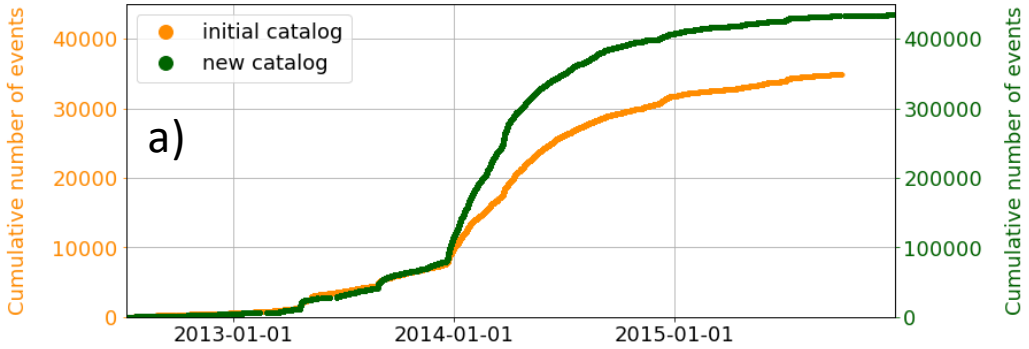

With **434,551** events **(CC > 12*MAD)**, the **enhanced catalog contains 12 times** more events than initially listed. The comparison of the events over time in a) (two y-scales) shows that features like accelerations in the initial catalog are preserved in the enhanced catalog.

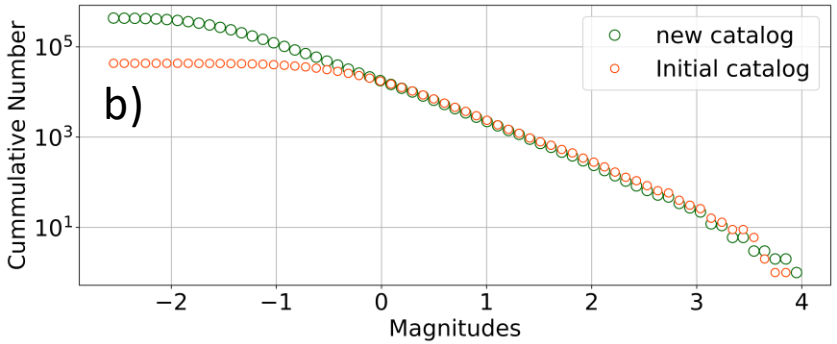

For the **magnitude estimation** of new detections we follow an approach based on **amplitude ratios** between the new detection and the template event (Ross et al., 2019).
Comparing the f**requency-magnitude distribution** of both catalogs in b) shows that with the detection approach used in this study the **additionally** detected events are mainly **small events (M < 0)**.

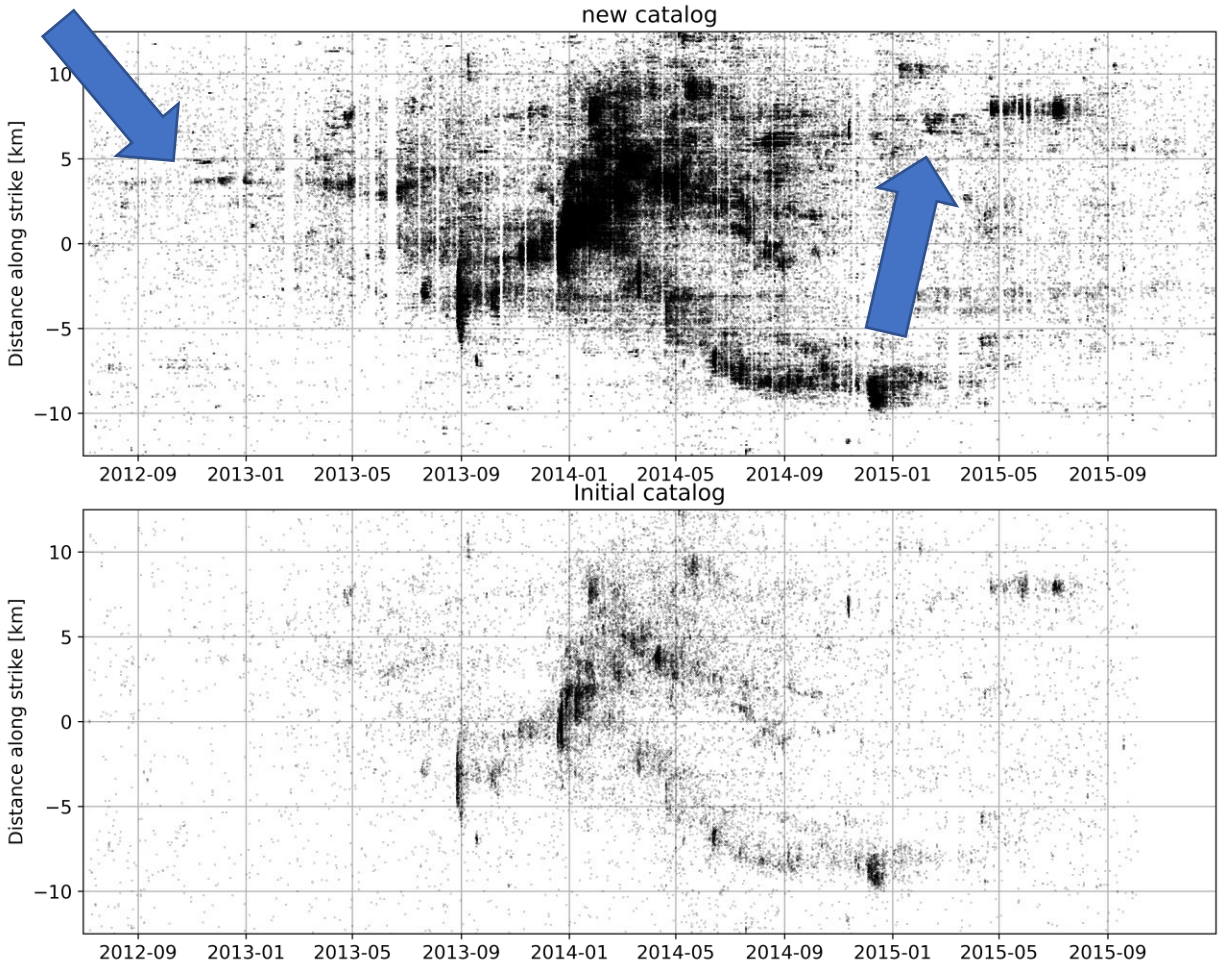

Comparing the spatio-temporal evolution of the seismicity (along strike taking the largest event of the sequence (M=3.81, 2013-12-22) as the center) shows that areas of increased seismicity within the initial catalog are preserved and amplified (in terms of number of events). Additionally, the new catalog reveals areas of increased seismicity which cannot be found in the initial catalog (indicated by arrows)

Results – Characterisation of the seismicity

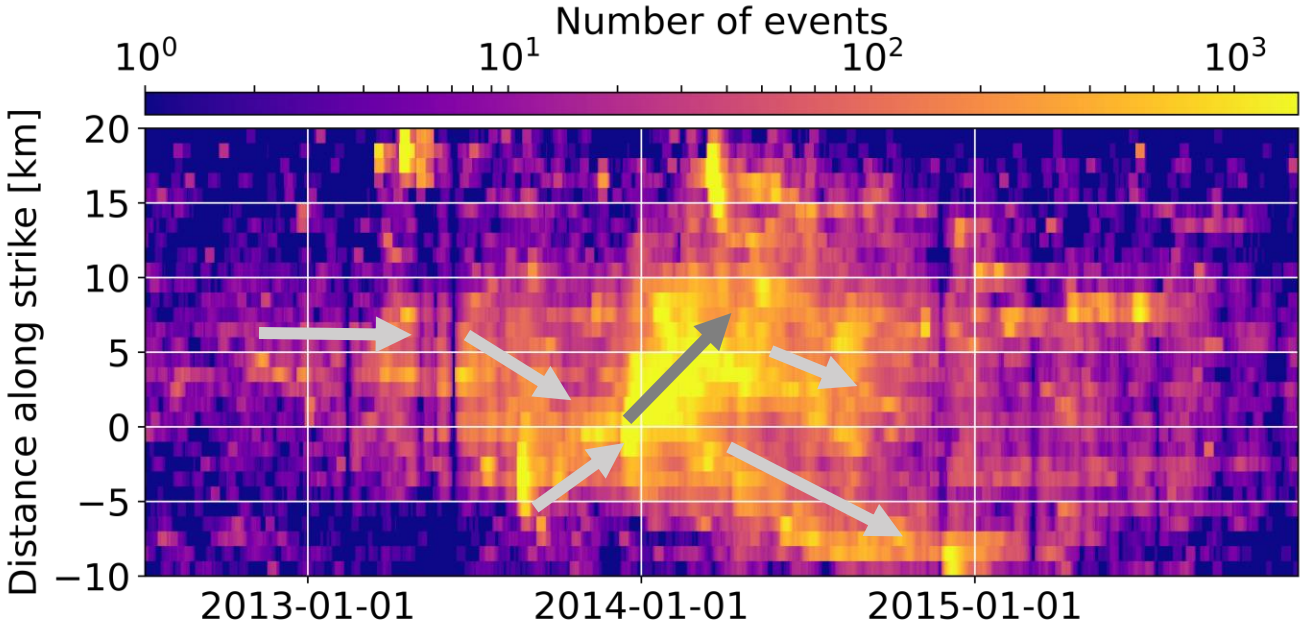

In order to analyze the spatio-temporal evolution of increased seismicity we binned the events in space (distinct distances along strike) and counted the number of events within a sliding window of 10 days (10% overlap). This Figure shows that the period of increased seismicity starts already in late 2012, early 2013 with an along-strike distance of around 5 km to the largest event of the sequence. In mid 2013 the **increased seismicity starts to migrate heterogeneously** over time along **distinct paths** which are highlighted by the arrows. Notably, the parallel migration along two distinct paths in late 2014.

Results – Characterization of the seismicity

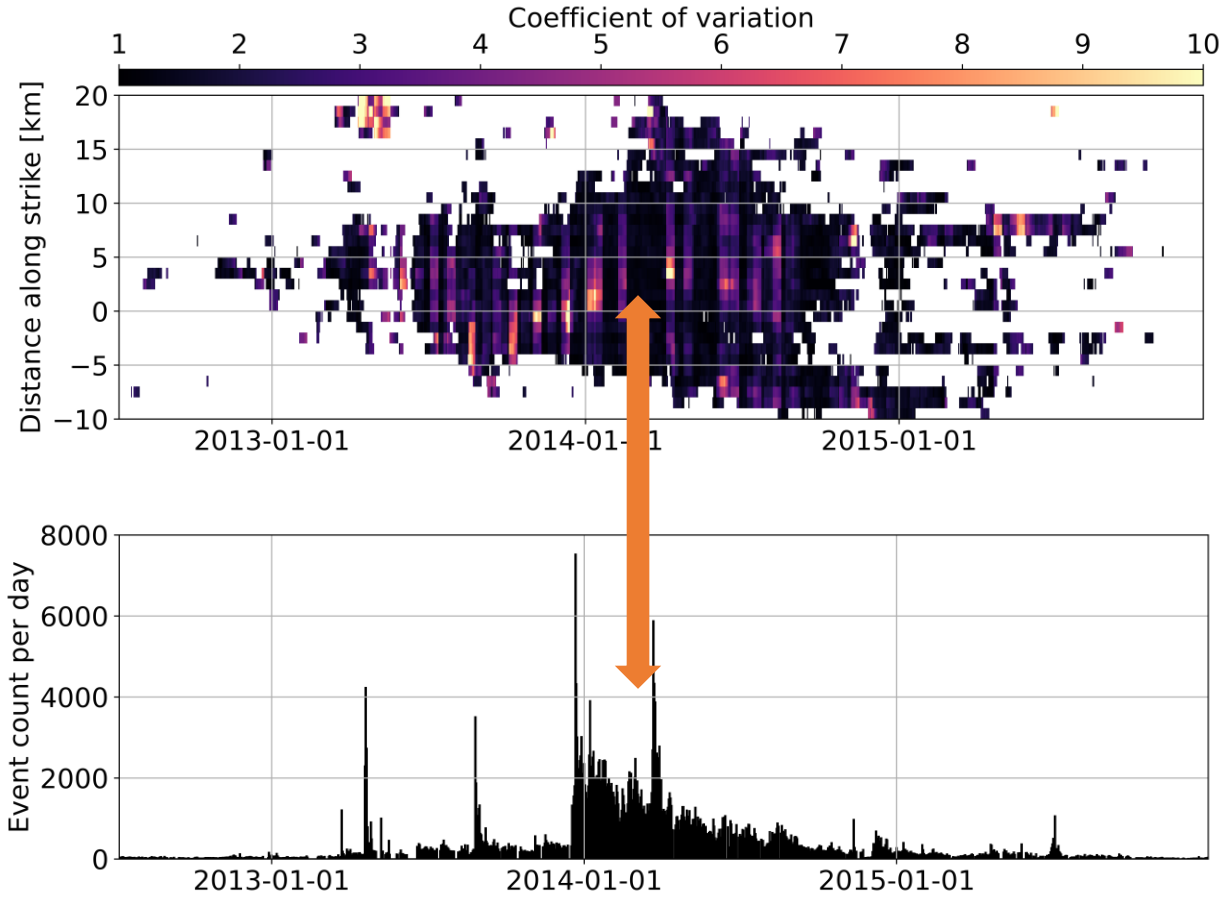

Using the approach explained in slide 7 we further calculate the **Coefficient of Variation** (COV) for every time window that contains more than 30 events in order to statistically characterize the seismicity along strike (see upper Figure). The **overall seismicity** exhibit **COV close to 1.** However, for a **small number of time windows** we find **COV >> 1.** These periods of COV >> 1 are **short in time** and **migrating along-strike.**

The lower Figure shows the event count per day over time. In early 2013 the number of events per day starts slightly to increase until late 2013 where a sudden change indicated by a large number of events per day can be seen. The large numbers of events per day are then fading out over time until the end of 2015.
This **overall trend** of seismicity is **intermittent** several times by punctuated peaks indicating a large number of events in a short period of time. These peaks **last up to several days** and some of them **coincide** in time with the largest events in the sequence.

Summarizing the two Figures reveals two main trends:

1. **COV ~ 1** for the **overall seismicity** (even for time periods with a large number of events, indicated by arrow)
2. punctual **COV >> 1** intermit the small COV values for **short time periods** and **migrate along-strike**

Conclusion

- The **combination** of **template matching** with seismic data from **borehole seismometers** helps to **extend** an existing catalog by a **factor > 12** (depending on the quality threshold)
  - Additional events
    - are mainly of small magnitudes (M < 0)
    - reveal additional small seismic bursts

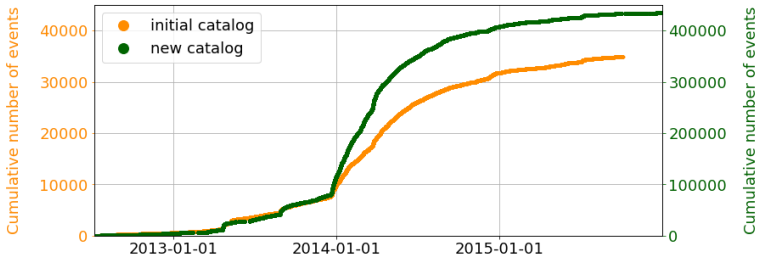

- The seismicity in the study area consist of at least **two trends**:
  1. **Long duration swarm-like sequence**
     - **COV ~ 1** indicating a **stationary process**
     - driven by external forcing (e.g. transient slip, fluid migration and redistribution)

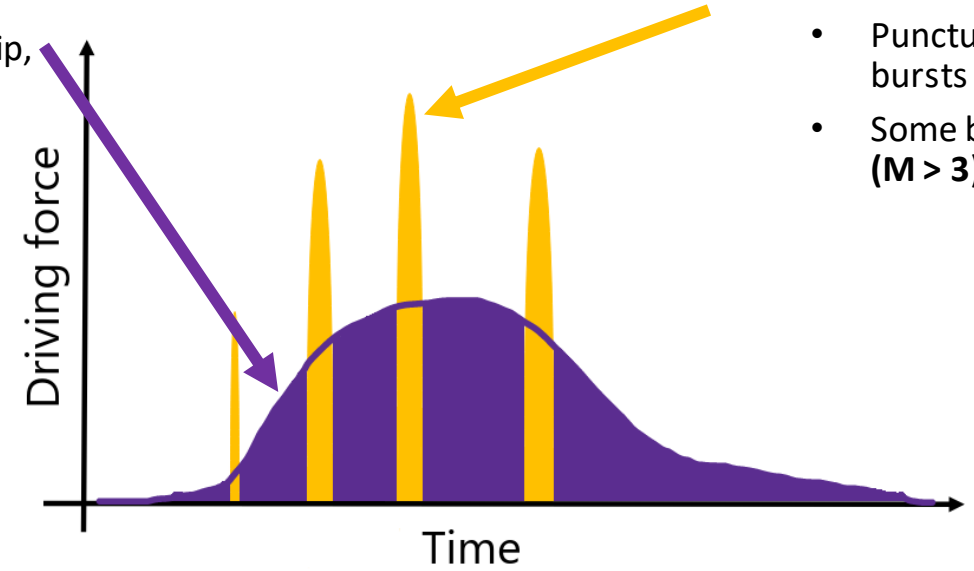

2. **Short duration peaks** (hours, days)
   - COV >> 1 suggesting **interacting seismicity**
   - Punctuated activation resulting in seismic bursts
   - Some bursts coincide with the **largest events (M > 3)** of the sequence

Outlook

- Further statistical characterization of the seismicity in time and space using
  - Fractal dimensions
  - b-values

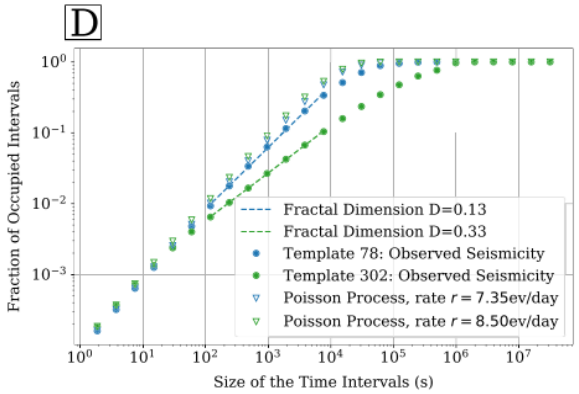

Beaucé, E et al. (2019)

- With the combination of GNSS and seismic data we will characterize the slow deformation in terms of small scale dynamics

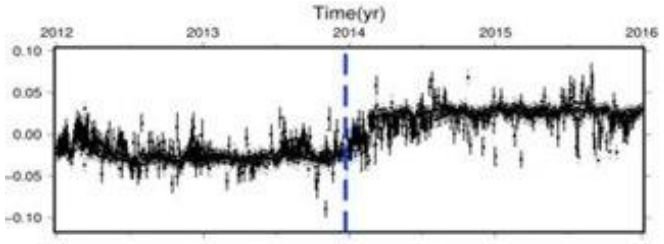

Gualandi, A et al. (2017)

References

- **Chiaraluce et al.**, Catalog of seismicity, 2019
- **Ross, Z. E**., Trugman, D. T., Hauksson, E., & Shearer, P. M. (2019). Searching for hidden earthquakes in Southern California. *Science*, *771*(May), 767–771
- **Anderlini, L**., Serpelloni, E., & Belardinelli, M. E. (2016). Creep and locking of a low-angle normal fault: Insights from the Altotiberina fault in the Northern Apennines (Italy). *Geophysical Research Letters*, *43*(9)
- **Gualandi et al.**, Aseismic deformation associated with an earthquake swarm in the northern Apennines (Italy), 2017
- **Beaucé, E.**, & Frank, W. B. (2018). *Fast Matched Filter (FMF): An Efficient Seismic Matched-Filter Search for Both CPU and GPU Architectures*. *89*(1)
- **Sánchez-Reyes, H.**, Essing, D., Beaucé, E., & Poli, P. (2020). *The imbricated foreshock and aftershock activities of the Balsorano (Italy) M w 4 . 4 normal fault earthquake and implications for earthquake initiation*. 1–15
- **Dresen, G.**, Kwiatek, G., Goebel, T., & Ben-Zion, Y. (2020). Seismic and Aseismic Preparatory Processes Before Large Stick–Slip Failure. *Pure and Applied Geophysics*, *177*, 5741–5760
- **Vadacca, L.**, Casarotti, E., Chiaraluce, L., & Cocco, M. (2016). On the mechanical behaviour of a low-angle normal fault: The Alto Tiberina fault (Northern Apennines, Italy) system case study. *Solid Earth*, *7*(6), 1537–1549